Shallow quantum circuits for efficient preparation of Slater determinants and correlated states on a quantum computer

Chong Hian Chee,[1,*] Daniel Leykam,[1] Adrian M. Mak,[2] and Dimitris G. Angelakis[1,3,4,†]

[1]*Centre for Quantum Technologies, National University of Singapore, 3 Science Drive 2, Singapore 117543*

[2]*Institute of High Performance Computing, Agency for Science, Technology & Research (A*STAR), 1 Fusionopolis Way, 16-16 Connexis, Singapore 138632*

[3]*School of Electrical and Computer Engineering, Technical University of Crete, 73100 Chania, Greece*

[4]*AngelQ Quantum Computing, 531A Upper Cross Street, 04-95 Hong Lim Complex, Singapore 051531*

(Received 25 January 2023; revised 23 May 2023; accepted 27 July 2023; published 18 August 2023)

Fermionic *Ansatz* state preparation is a critical subroutine in many quantum algorithms such as the variational quantum eigensolver for quantum chemistry and condensed-matter applications. The shallowest circuit depth needed to prepare Slater determinants and correlated states to date scales at least linearly with respect to the system size N. Inspired by data-loading circuits developed for quantum machine learning, we propose an alternate paradigm that provides shallower, yet scalable, $O(d \log_2^2 N)$ two-qubit gate-depth circuits to prepare such states with d fermions, offering a subexponential reduction in N over existing approaches in second quantization, enabling high-accuracy studies of $d \ll O(N/\log_2^2 N)$ fermionic systems with larger basis sets on near-term quantum devices.

DOI: 10.1103/PhysRevA.108.022416

I. INTRODUCTION

Quantum computers promise the ability to solve hard many-body problems in quantum chemistry and condensed-matter physics, including the computation of ground-state energies and simulation of quantum dynamics [1–3]. The relevant quantum algorithms frequently involve quantum state preparation as a key step. For example, the success probability of quantum phase estimation is determined by the overlap of a trial *Ansatz* state with the eigenstate of interest [4–6]. Thus, efficient preparation of high-quality *Ansatz* states is crucial for many-body applications of quantum computing [7,8].

Most existing methods for preparing fermionic *Ansätze* use second quantization with Jordan-Wigner mapping [9] to efficiently represent the quantum many-body fermionic wavefunction using a number of qubits that scales linearly in the system size [1,2]. Widely-used fermionic *Ansätze* typically fall into two broad classes: The first class consists of hardware-efficient *Ansätze* which use parameterized hardware-native gates to minimize the depth of the quantum circuit [10], but are difficult to optimize [11] and do not guarantee an accurate representation of the desired quantum state [12]. The second class consists of problem-inspired *Ansätze* which are more promising and explicitly incorporate the physics of the system of interest, but require deeper circuits that scale polynomially in system size, which exacerbates errors due to quantum noise and decoherence [13–20], limiting state-of-the-art demonstrations to less than a hundred qubits [21,22], leaving studies of chemically-relevant molecular systems requiring more than 10^2–10^3 qubits well out of reach [23,24].

The shallowest general-purpose problem-inspired *Ansatz* states to date are mean-field Hartree-Fock states [13–15], which are Slater determinants that can be prepared using a mesh of fermionic single-excitation gates which have a linear $O(N)$ two-qubit gate depth in the number of qubits N, as shown in Fig. 1(a). While Hartree-Fock states are efficiently simulatable using classical computers, they nevertheless serve as a useful starting point for quantum computers to prepare more interesting classically intractable correlated quantum *Ansätze*, such as the unitary coupled-cluster *Ansatz*, which incorporates quantum correlations by applying number-conserving multifermion excitation operators to a reference Hartree-Fock state [16–20,25].

Fermionic excitation operators are examples of Givens-rotation gates which perform rotations in a two-dimensional fermionic subspace of a larger Hilbert space and, together with their controlled variants, form a universal quantum gate set to realize any particle-conserving unitaries [26,27]. Therefore, such Givens-rotation gates have been helpful for preparing various fermionic states in quantum chemistry and condensed-matter applications [13–17,28–30]. Recently, such gates have also attracted interest in the context of quantum linear algebra, where they were used to construct shallow-depth "Clifford-loader" gates, which are linear combinations of anticommuting operators, as a means to efficiently encode d-dimensional subspaces of $\mathbb{R}^N$ into an N-qubit state [31–34], enabling potential end-to-end quantum speedups for several quantum machine learning and linear-algebra problems, including determinant sampling and topological data analysis [31]. It is thus timely to consider whether the implementation of Clifford loaders via the Givens rotation is useful for preparing fermionic *Ansatz* states.

*ch.chee@u.nus.edu

†dimitris.angelakis@gmail.com

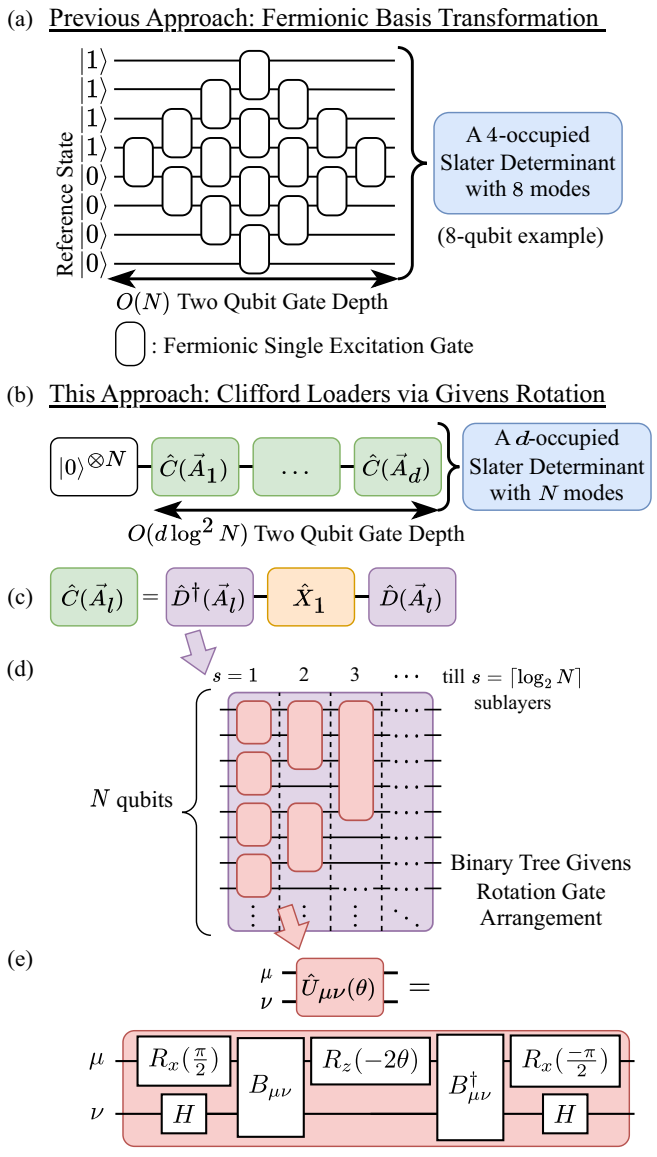

FIG. 1. Different approaches for preparing d-occupied Slater determinants of N modes on a quantum computer, assuming Jordan-Wigner mapping. (a) Existing approaches use a linear-depth mesh of fermionic single-excitation gates to apply a fermionic basis transformation to a reference state [13–15]. (b) The proposed Clifford loaders via the Givens-rotation approach applies a sequence $\hat{C}$ of gates d times to an all-zero state of N qubits $|0\rangle^{\otimes N}$. (c) $\hat{C}$ consists of two products of multiple Givens rotations, $\hat{D}$ and $\hat{D}^\dagger$, that sandwich a Pauli-X gate on the first qubit. (d) The Givens rotations $\hat{U}_{\mu\nu}$ are arranged in a binary tree. (e) $\hat{U}_{\mu\nu}$ is decomposed using Pauli rotation gates R_x and R_z acting on qubit μ, Hadamard gates H acting on qubit ν, and CNOT ladders $B_{\mu\nu}$ acting on all qubits between μ and ν. θ and $\vec{A}$ are scalar and vector parameters, respectively.

Here, we shall show how a d-fermion Slater determinant can be prepared in second quantization using Clifford loaders with an overall $O(d \log_2 N)$ Givens-rotation gate depth. An overall $O(d \log_2^2 N)$ two-qubit gate-depth scaling is thus achieved using Givens-rotation gates with $O(\log_2 N)$ two-qubit gate depth under Jordan-Wigner fermion-to-qubit mapping. This is more depth efficient than existing approaches that scale as $O(N)$ in two-qubit gate depth with respect to the system size N for a sufficiently slowly growing d. We also show how this approach can be extended using the same preparation technique for Slater determinants to prepare fermionic L-wise correlated *Ansatz* states, which correlate between L-tuples of the fermionic modes in the *Ansatz*, to get quantum circuits that are shallower than that of the Slater determinant by at least a factor of L. Finally, to validate our correlated *Ansatz*, we shall demonstrate how the $L = 2$ pairwise correlated *Ansatz* can be used to capture a significant fraction of correlation energy using an example of hydrogen chains up to $N = 20$ qubits, for which pairwise electronic correlation is likely to be significant. Our results establish Clifford loaders constructed out of Givens rotations as a promising method for efficient, practical, and scalable preparation of fermionic *Ansatz* states for large quantum chemistry applications on near-term quantum computers.

II. PREPARING SLATER DETERMINANTS USING SHALLOW CIRCUITS

We begin by showing how a Slater determinant with d occupied and $N - d$ unoccupied fermionic modes can be prepared using a shallow quantum circuit. An arbitrary Slater determinant $|\Psi_1\rangle$ is defined as [13,35–37]

$$|\Psi_1(A)\rangle := \prod_{l=1}^{d} \sum_{\mu=1}^{N} A_{\mu l} \hat{a}_\mu^\dagger |\text{vac}\rangle, \tag{1}$$

where A is an $N \times d$ real matrix such that all d columns are orthogonal and normalized, $|\text{vac}\rangle$ is a vacuum state, and $\hat{a}_\mu^\dagger$ is a creation operator acting on the μth mode. While the definition in Eq. (1) is pedagogically convenient, it requires nonunitary operators $\Sigma_{\mu=1}^{N} A_{\mu l} \hat{a}_\mu^\dagger$ which cannot be directly implemented on a quantum circuit. Consequently, the most efficient method to prepare Slater determinants to date is to perform a fermionic basis transformation to a reference Slater-determinant state for a given skew-Hermitian parameter matrix κ as

$$|\Psi_1(A)\rangle = \exp\left[\sum_{\mu,\nu=1}^{N} \kappa_{\mu\nu} \hat{a}_\mu^\dagger \hat{a}_\nu\right] \prod_{r=1}^{d} a_r^\dagger |\text{vac}\rangle, \tag{2}$$

where the fermionic basis transformation is implemented as a linear-depth mesh of fermionic single-excitation gates $\exp[\theta(\hat{a}_\mu^\dagger \hat{a}_\nu - \hat{a}_\nu^\dagger \hat{a}_\mu)]$, as shown in Fig. 1(a) [14,15].

We propose to improve the circuit-depth efficiency of preparing Slater determinants using the equivalent form

$$|\Psi_1(A)\rangle := \prod_{l=1}^{d} \sum_{\mu=1}^{N} A_{\mu l} \hat{p}_\mu |\text{vac}\rangle, \tag{3}$$

as shown in Appendix A, where we use anticommuting operators

$$\hat{p}_\mu = \hat{a}_\mu^\dagger + \hat{a}_\mu, \tag{4}$$

with the relation $\{\hat{p}_\mu, \hat{p}_\nu\} = 2\delta_{\mu\nu}\mathbf{I}$, as shown in Appendix B. Using the anticommuting operators $\hat{p}_\mu$ instead of $\hat{a}_\mu^\dagger$ allows us to exploit the recent result in Ref. [31] that provides a shallow $O(d \log_2 N)$ Givens-rotation gate-depth decomposition of the

Clifford loader

$$\hat{C}(\vec{A}_l) = \sum_{\mu=1}^{N} A_{\mu l}\hat{p}_\mu \tag{5}$$

for some normalized column $\vec{A}_l$. Applying the Clifford loaders $\hat{C}(\vec{A}_l)$ in succession d times on a vacuum state $|\text{vac}\rangle$, each with orthogonal columns $\vec{A}_l$, $l = 1, \ldots, d$, from matrix A generates the desired Slater determinant

$$|\Psi_1(A)\rangle = \prod_{l=1}^{d} \hat{C}(\vec{A}_l)|\text{vac}\rangle, \tag{6}$$

as shown in Fig. 1(b). In the case of $d > \frac{N}{2}$, we may apply the Clifford loader $N - d$ times instead, followed by occupation-vacant mode swap to all Fock bases at the end, which is equivalent to a Pauli-X bit flip to all qubits under the Jordan-Wigner mapping. The Slater determinant in Eq. (6) can be simplified to [31,38]

$$|\Psi_1(A)\rangle = \sum_{|B|=d} \det(A_B)|B\rangle, \tag{7}$$

where the sum is over all possible combinations of the ordered set B containing d unique integers from 1 to N, A_B is a $d \times d$ matrix minor of A whose row indexes are restricted by B, and $|B\rangle$ denotes an N-mode Fock basis with occupied modes indexed by B, as shown in Appendix C.

The Clifford loader $\hat{C}(\vec{A}_l)$ in Eq. (5) can be decomposed as

$$\hat{C}(\vec{A}_l) = \hat{D}(\vec{A}_l)\hat{p}_1\hat{D}^\dagger(\vec{A}_l), \tag{8}$$

as shown in Fig. 1(c), where the operator $\hat{p}_1 = \hat{a}_1^\dagger + \hat{a}_1$ acting on the first mode is sandwiched by two products of multiple Givens rotations, termed elsewhere as unary data loaders $\hat{D}$ [31,34,39]. Its conjugate transpose $\hat{D}^\dagger$ is expressed as

$$\hat{D}^\dagger(\vec{A}_l) = \prod_{s=1}^{\lceil \log_2 N \rceil} \left[\prod_{\mu,\nu\in\mathfrak{T}_s} \hat{U}_{\mu\nu}\left(\theta_{\mu\nu}^{(sl)}\right) \right], \tag{9}$$

where the Givens rotations

$$\hat{U}_{\mu\nu}(\theta) = \exp[\theta\hat{p}_\mu\hat{p}_\nu] \tag{10}$$

are arranged in a binary-tree pattern according to the set of (μ, ν) indexes $\mathfrak{T}_s = \{(\mu,\nu)|\mu = 2^s(k-1)+1,\ \nu = 2^{s-1}(2k-1)+1,\ k \in \mathbb{Z}^+\backslash 0\}$ for each sublayer $s\in\{1, \ldots, \lceil \log_2 N\rceil\}$, as shown in Fig. 1(d).

By treating $\vec{A}_l = (A_{1l}, \ldots, A_{Nl})$ in Eq. (9) as a vector in the basis of $\{\hat{p}_1, \ldots, \hat{p}_N\}$, we exploit the Givens-rotation property that

$$\hat{U}_{\mu\nu}(\theta)\hat{p}_r\hat{U}_{\mu\nu}^\dagger(\theta) = \begin{cases} \cos(2\theta)\hat{p}_r + \sin(2\theta)\hat{p}_\nu & r = \mu, \\ \cos(2\theta)\hat{p}_r - \sin(2\theta)\hat{p}_\mu & r = \nu, \\ \hat{p}_r & r \neq \mu, \nu, \end{cases} \tag{11}$$

to obtain the required rotation angles $\theta_{\mu\nu}^{(sl)} = \frac{1}{2}\arctan\frac{A_{\nu l}^s}{A_{\mu l}^s}$ classically by numerically performing parallel Givens rotations on $\vec{A}_l$ that correspond to the sequence in $\hat{D}^\dagger$ that successively zeros out the vector elements until the first element of $\vec{A}_l$ becomes $A_{1l} = 1$, corresponding to $\hat{p}_1$.

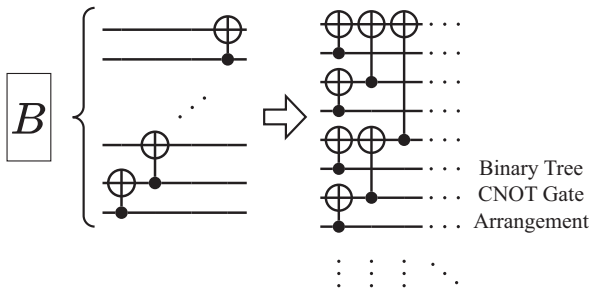

FIG. 2. Linear-depth cascading CNOT ladder B in the decomposition of the Givens-rotation gate $\hat{U}$ is replaced by a nonequivalent logarithmic-depth circuit that has no effect on $\hat{U}$.

Under the Jordan-Wigner mapping, the Givens rotation in Eq. (10) maps to $\exp[-i\theta\hat{Y}_\mu\hat{X}_\nu\otimes_{r=\mu+1}^{\nu-1}\hat{Z}_r]$, which is a Pauli-string rotation gate that can easily be implemented on a quantum circuit [28,40], as shown in Fig. 1(e). The controlled-NOT (CNOT) ladder $B_{\mu\nu}$ in the gate decomposition of the Givens rotation $\hat{U}_{\mu\nu}$ serves the purpose of encoding the parity of nonexciting qubits into the rotation gate, and it consists of a cascade of CNOT gates [28,40]. However, this CNOT ladder can be replaced by the nonequivalent binary-tree CNOT gate arrangement [31] shown in Fig. 2, without any effect on the Givens rotation $\hat{U}_{\mu\nu}$, thereby reducing the CNOT depth from linear to logarithmic in N. Thus, by implementing d such Clifford loaders with these Givens-rotation gates, we can prepare Slater determinants with shallow $O(d\log_2^2 N)$ two-qubit gate-depth quantum circuits.

III. EXTENSION TO A CORRELATED *ANSATZ*

Next, we extended the technique above by introducing a method to incorporate L-wise correlations into the fermionic *Ansatz* state preparation, where $L = 1$ reduces to the Slater-determinant case. The idea is to use a set of anticommuting operators that contains non-particle-preserving multibody Fock operators for the Clifford loaders in Eq. (5) and apply the same technique undertaken in the Slater-determinant case. Here, for simplicity we work with Pauli-string operators under the Jordan-Wigner mapping. We extend the anticommuting operator $\hat{p}_\mu = \bigotimes_{r=1}^{\mu-1}\hat{Z}_r\hat{X}_\mu$ used to prepare the Slater determinant previously to

$$\hat{p}_\mu^{(L)} = \bigotimes_{r=1}^{\mu-1}\hat{Z}_{rL} \bigotimes_{r'=L(\mu-1)+1}^{\mu L}\hat{X}_{r'} \tag{12}$$

to generate L-wise correlations. The modified operator $\hat{p}_\mu^{(L)}$ has L Pauli-X terms and μ Pauli-Z terms with modulo L indexes such that $\hat{p}_\mu^{(L)}$ remains anticommuting $\{\hat{p}_\mu^{(L)}, \hat{p}_\nu^{(L)}\} = 2\delta_{\mu\nu}\mathbf{I}$, as shown in Appendix B. For example, the $L = 2$ pairwise correlated anticommuting operator is given as $\hat{p}_\mu^{(2)} = \hat{Z}_2\hat{Z}_4\hat{Z}_6\cdots\hat{Z}_{2\mu-2}\hat{X}_{2\mu-1}\hat{X}_{2\mu}$. Thus, we may prepare an N-mode d-occupied L-wise correlated state $|\Psi_L\rangle$ by applying $\frac{d}{L}$ Clifford loaders $\hat{C}_L$,

$$|\Psi_L(G)\rangle = \prod_{l=1}^{\frac{d}{L}}\hat{C}_L(\vec{G}_l)|\text{vac}\rangle, \tag{13}$$

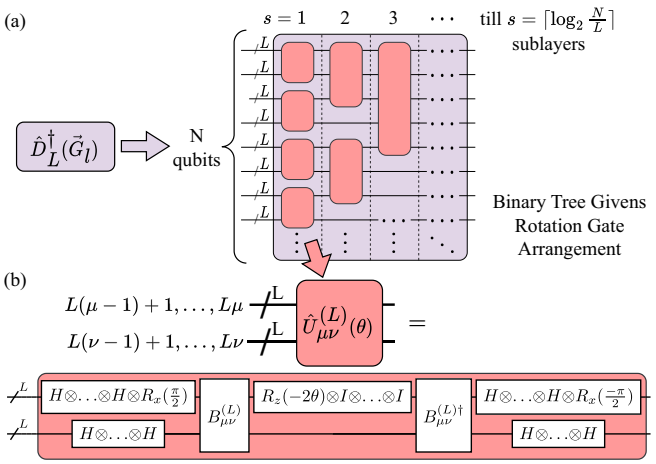

FIG. 3. (a) A product of multiple Givens rotations $\hat{D}_L^\dagger$ that is composed of Givens-rotation gates $\hat{U}_{\mu,\nu}^{(L)}$ in a binary-tree arrangement on the quantum circuit. (b) $\hat{U}_{\mu,\nu}^{(L)}$ is decomposed using Pauli rotation gates R_x, acting on qubit $L\mu$, and R_z, acting on qubit $L(\mu-1)+1$, and Hadamard gates H and CNOT ladders $B_{\mu\nu}^{(L)}$ that act on all $2L-1$ qubits in $\{L(\mu-1)+1, \ldots, L\mu-1\}$ and $\{L(\nu-1)+1, \ldots, L\nu\}$, with $B_{\mu\nu}^{(L)}$ also acting on $\nu-\mu$ additional qubits in $\{L\mu, L(\mu+1), L(\mu+2), \ldots, L(\nu-1)\}$. θ and $\vec{G}$ are scalar and vector parameters, respectively.

where G is an $\frac{N}{L} \times \frac{d}{L}$ orthonormal matrix and $\vec{G}_l$ is a column vector of G, which simplifies to

$$|\Psi_L(G)\rangle \simeq \sum_{|B'|=\frac{d}{L}} \det(G_{B'})|B'_L\rangle \tag{14}$$

up to an unobserved global phase, where the sum is over all combinations of the ordered set B' containing $\frac{d}{L}$ unique integers between 1 and $\frac{N}{L}$, $G_{B'}$ is a $\frac{d}{L} \times \frac{d}{L}$ matrix minor of G whose rows are restricted to B', $B'_L = \{L(j-1)+1, L(j-1)+2, \ldots, Lj | j \in B'\}$, and $|B'_L\rangle$ denotes an N-mode Fock state with occupied modes indexed by B'_L, as shown in Appendix C.

The L-wise correlated *Ansatz* state $|\Psi_L\rangle$ in Eq. (14) is similar to the Slater determinant $|\Psi_1\rangle$ from Eq. (7) with regard to how the amplitudes are calculated but differs in the Fock states that have nonzero amplitudes. In the Slater-determinant case, all Fock states with particle number d will have nonzero amplitudes, while in the $L=2$ pairwise case, all Fock states that have both particle number d and $L=2$-tuple neighboring occupations and neighboring vacancies will have nonzero amplitudes. For instance, in the case $N=4$ and $d=2$, Fock states $\{|0011\rangle, |1100\rangle\}$ will have nonzero amplitudes, and $\{|0101\rangle, |0110\rangle, |1010\rangle, |1001\rangle\}$ will have zero amplitudes.

For a given normalized column $\vec{G}_l$, we may define a corresponding L-wise correlated Clifford loader $\hat{C}_L(\vec{G}_l) = \hat{D}_L^\dagger(\vec{G}_l)\hat{p}_1^{(L)}\hat{D}_L(\vec{G}_l)$, where $\hat{p}_1^{(L)} = \bigotimes_{r=1}^{L} \hat{X}_r$ consists of L Pauli-X gates that act on the first L qubits sandwiched by two products of multiple Givens rotations, $\hat{D}_L$ and $\hat{D}_L^\dagger$. Each $\hat{D}_L$ is composed of Givens-rotation gates $\hat{U}_{\mu\nu}^{(L)}(\theta) = \exp[\theta \hat{p}_\mu^{(L)} \hat{p}_\nu^{(L)}]$ arranged in a binary-tree pattern similar to that shown in Fig. 3(a). Since the Givens-rotation gate $\hat{U}_{\mu\nu}^{(L)}(\theta)$ is a Pauli-string rotation gate, its gate decomposition [40] and the corresponding rotation angle can be obtained in a fashion similar to that in the Slater-determinant case, as shown Fig. 3(b). We refer readers to Appendix D for the explicit form of the Givens rotation in terms of Pauli operators.

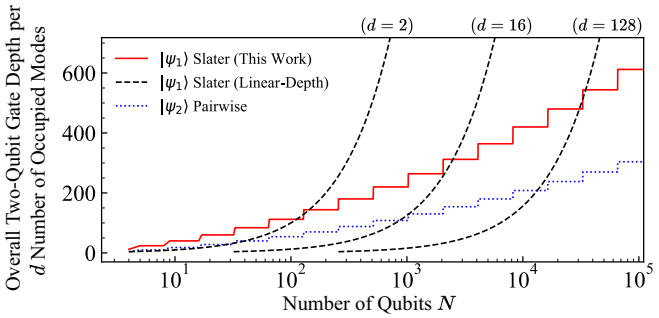

FIG. 4. Estimated two-qubit gate depth per occupied mode d to prepare an N-mode Slater determinant $|\Psi_1\rangle$ and an $L=2$ pairwise correlated *Ansatz* state $|\Psi_2\rangle$ using Clifford loaders compared to existing d-independent linear-depth approaches.

IV. RESOURCE ANALYSIS

For simplicity, we treat all types of two-qubit gate depths as equal and assume there is no circuit compilation. We estimated that the overall two-qubit gate depth required to prepare an L-wise correlated *Ansatz* state $|\Psi_L\rangle$ is $\frac{2d}{L}\{\lceil \log_2^2 \frac{N}{L} \rceil + (1+2\log_2 L)\lceil \log_2 \frac{N}{L} \rceil\} \approx O(\frac{d}{L}\log_2^2 \frac{N}{L})$, as shown in Appendix E. This shows that our approach to prepare an L-wise correlated *Ansatz* state $|\Psi_L\rangle$ is shallower than a Slater determinant $|\Psi_1\rangle$ by at least a factor of L, *ceteris paribus*.

We plotted the estimated two-qubit gate depth per occupied mode for Slater determinants $|\Psi_1\rangle$ and pairwise correlated *Ansatz* states $|\Psi_2\rangle$ on a quantum computer, as shown in Fig. 4, and compared the result to the previous linear-depth approach of preparing $d=2$, 16, and 128 occupied Slater determinants, which has a d-independent two-qubit gate depth of about $2N$ [13–15]. Indeed, the crossover point $d \approx \frac{N}{\log_2^2 N}$ shows that the minimum number of qubits N required to achieve a shallower circuit increases subexponentially with the number of occupied modes d. However, we highlight that this crossover point can be practically surpassed by near-term quantum devices such as superconducting qubits [41] and trapped ions [42] with fewer than 10^5 qubits for systems with $2 \leqslant d \leqslant 128$ occupied fermionic modes, which is a sizable range that encompasses many systems of interest in quantum chemistry and condensed-matter physics. In general, our approach is suitable for problem classes that have a sufficiently slowly growing $d \ll O(\frac{N}{\log_2^2 N})$. One such problem is the computation of quantum observable quantities for fermionic systems for the complete-basis-set limit, where d is preserved but said quantities are computed for increasing values of N and extrapolated using various schemes to very large limits of N [43–45].

V. EXAMPLE: LINEAR HYDROGEN MOLECULAR CHAINS

To validate our $L=2$ pairwise correlated *Ansatz* state, we numerically evaluated the fraction of the electronic correlation energy $E_{\text{pair}}/E_{\text{corr}}$ captured by the optimized

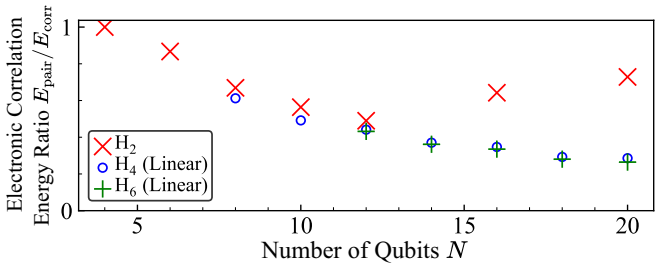

FIG. 5. Numerically calculated fraction of the electronic correlation energy ratio $E_{\text{pair}}/E_{\text{corr}}$ captured by an optimized pairwise correlated *Ansatz* state for hydrogen chains up to H_6 at a fixed interatomic distance of 1.4 bohrs for various basis-set mixtures up to 20 qubits.

pairwise correlated *Ansatz* state $|\Psi_2(G^*)\rangle$ for three linear hydrogen molecular chains (H_2, H_4, and H_6) with $d = 2$, 4, and 6 electrons at a fixed interatomic distance of 1.4 bohrs, where the pairwise electronic correlation is likely to be significant. $E_{\text{pair}} = E_{\text{HF}} - \langle \hat{H}_e \rangle$ is the correlation energy beyond the mean-field energy E_{HF} of a molecule captured by $|\Psi_2(G^*)\rangle$, while $E_{\text{corr}} = E_{\text{HF}} - E_{\text{FCI}}$ is the exact value of the correlation energy, where E_{FCI} is known as the full-configuration-interaction (FCI) energy. G^* is an optimized parameter matrix, obtained using a classical quasi-Newton Limited-memory Broyden-Fletcher-Goldfarb-Shanno algorithm with Bound constraints (L-BFGS-B) optimizer that minimizes the expectation of the electronic Hamiltonian $\langle \hat{H}_e \rangle$. We considered different mixtures of atomic basis sets [24], slater-type orbital approximated by 3 Gaussian primitives (STO-3G), split-valence (6-31G, 6-311G), correlation-consistent polarized valence double zeta (cc-pVDZ), augmented correlation-consistent polarized valence double zeta (aug-cc-pVDZ) for each hydrogen atom, resulting in system sizes ranging from 4 to 20 qubits. Such mixing of basis sets for each atom is a common strategy in computational quantum chemistry to reduce the resources required to achieve a desired precision [46]. All calculations were performed numerically using SCIPY [47], PYSCF [48], and PENNYLANE [49]. Figure 5 shows that a large fraction of the electronic correlation energy $E_{\text{pair}}/E_{\text{corr}}$ is captured by the optimized pairwise correlated *Ansatz* state $|\Psi_2(G^*)\rangle$.

VI. SUMMARY AND OUTLOOK

We proposed Givens-rotation-based Clifford loaders for efficient preparation of d occupied Slater determinants $|\Psi_1\rangle$ of N modes using shallower $O(d \log_2^2 N)$ two-qubit gate-depth quantum circuits. We also showed that by redefining new sets of the anticommutation operators $\hat{p}_\mu$ for the Clifford loaders, the same technique can be used to prepare L-wise correlated *Ansatz* states $|\Psi_L\rangle$ to yield quantum circuits shallower than those of Slater determinants by at least a factor of L. As demonstrated in the application of $L = 2$ pairwise correlated *Ansatz* states to hydrogen chains, L-wise correlated states are potentially useful in fermionic systems with significant L-wise fermionic correlation, even though they are not expected to fully capture all the correlation energy. It will be interesting to generalize the Clifford loaders to other types of fermionic correlation while keeping the same shallow gate-depth scaling intact.

To the best of our knowledge, our approach to fermionic *Ansatz* state preparation offers a subexponential improvement in gate depth over existing methods in the second quantization with respect to system size N for fermionic problems where the number of occupied modes is $d \ll O(\frac{N}{\log_2^2 N})$. Nonetheless, our results have established Clifford loaders via Givens rotations as an efficient, yet practical and scalable, fermionic *Ansatz* state-preparation technique, which will enable the study of molecules and materials requiring larger basis-set sizes on near-term quantum devices.

ACKNOWLEDGMENTS

This research is supported by the National Research Foundation, Singapore, and A*STAR under its CQT Bridging Grant and Quantum Engineering Programme, Grant No. NRF2021-QEP2-02-P02, A*STAR (No. 21709), and by the European Union's Horizon Programme (HORIZON-CL4-2021-DIGITALEMERGING-02-10), Grant Agreement No. 101080085, QCFD.

APPENDIX A: PROOF OF EQUIVALENCE BETWEEN TWO DEFINITIONS OF AN ARBITRARY SLATER DETERMINANT

An arbitrary Slater determinant $|\Psi_1(A)\rangle$ with d occupied and $N - d$ unoccupied fermionic modes is defined as

$$|\Psi_1(A)\rangle = \prod_{l=1}^{d} \sum_{k=1}^{N} A_{lk} \hat{a}_k^\dagger |\text{vac}\rangle, \tag{A1}$$

where A is an $N \times d$ real matrix such that all the d columns are orthogonal and normalized, $|\text{vac}\rangle$ is a vacuum state, and $\hat{a}_k^\dagger$ is a creation operator acting on the kth mode. To begin, we expand the product in Eq. (A1) and replace the index k in the summation with indices $k_1, \ldots, k_d$,

$$|\Psi_1(A)\rangle = \left(\sum_{k_d=1}^{N} A_{dk_d} \hat{a}_{k_d}^\dagger \right) \cdots \left(\sum_{k_1=1}^{N} A_{1k_1} \hat{a}_{k_1}^\dagger \right) |\text{vac}\rangle \tag{A2}$$

$$= \sum_{k_d,\ldots,k_1=1}^{N} A_{dk_d} \cdots A_{1k_1} \hat{a}_{k_d}^\dagger \cdots \hat{a}_{k_1}^\dagger |\text{vac}\rangle. \tag{A3}$$

We want to show that Eq. (A3) is equivalent to the alternate definition of the Slater determinant,

$$|\Psi_{1,\text{alt}}(A)\rangle = \prod_{l=1}^{d} \sum_{k=1}^{N} A_{lk} (\hat{a}_k^\dagger + \hat{a}_k) |\text{vac}\rangle, \tag{A4}$$

where we use an anticommuting operator $\hat{a}_k^\dagger + \hat{a}_k$. Starting from Eq. (A4), we expand the product and replace index k in the summation with indices $k_1, \ldots, k_d$,

$$|\Psi_{1,\text{alt}}(A)\rangle = \left(\sum_{k_d=1}^{N} A_{dk_d} (\hat{a}_{k_d}^\dagger + \hat{a}_{k_d}) \right) \cdots \left(\sum_{k_1=1}^{N} A_{1k_1} (\hat{a}_{k_1}^\dagger + \hat{a}_{k_1}) \right) |\text{vac}\rangle. \tag{A5}$$

Here, we consider evaluating the product of the two rightmost summation terms in Eq. (A5). We split the derivation into two cases, $d = 1$ and $d > 1$. For $d = 1$, we note that $\hat{a}_j|\text{vac}\rangle = 0$ for any mode j; thus, Eqs. (A3) and (A5) become trivially equivalent. For $d > 1$ we have,

$$\left[\sum_{k_2=1}^{N} A_{2k_2}(\hat{a}_{k_2}^\dagger + \hat{a}_{k_2})\right]\left[\sum_{k_1=1}^{N} A_{1k_1}(\hat{a}_{k_1}^\dagger + \hat{a}_{k_1})\right]$$

$$= \sum_{k_2,k_1=1}^{N} A_{2k_2}A_{1k_1}(\hat{a}_{k_2}^\dagger + \hat{a}_{k_2})\big(\hat{a}_{k_1}^\dagger + \hat{a}_{k_1}\big) \tag{A6}$$

$$= \sum_{k_2,k_1=1}^{N} A_{2k_2}A_{1k_1}\big(\hat{a}_{k_2}^\dagger\hat{a}_{k_1}^\dagger + \hat{a}_{k_2}^\dagger\hat{a}_{k_1} + \hat{a}_{k_2}\hat{a}_{k_1}^\dagger + \hat{a}_{k_2}\hat{a}_{k_1}\big). \tag{A7}$$

We then apply the fermionic commutation relation $\{\hat{a}_\alpha, \hat{a}_\beta^\dagger\} = \delta_{\alpha\beta}\mathbf{I}$ to Eq. (A7) to get

$$\sum_{k_2,k_1=1}^{N} A_{2k_2}A_{1k_1}\big(\hat{a}_{k_2}^\dagger\hat{a}_{k_1}^\dagger + \delta_{k_2k_1}\mathbf{I} + \hat{a}_{k_2}\hat{a}_{k_1}\big), \tag{A8}$$

and since the columns of A are orthogonal, the inner product between any column i, j vanishes, $\sum_k A_{ik}A_{jk} = 0$, and we thus have

$$\sum_{k_2,k_1=1}^{N} A_{2k_2}A_{1k_1}\big(\hat{a}_{k_2}^\dagger\hat{a}_{k_1}^\dagger + \hat{a}_{k_2}\hat{a}_{k_1}\big). \tag{A9}$$

Substituting Eq. (A9) back into Eq. (A5) and using $\hat{a}_j|\text{vac}\rangle = 0$ for any mode j gives

$$|\Psi_{1,\text{alt}}(A)\rangle = \left(\sum_{k_d=1}^{N} A_{dk_d}\big(\hat{a}_{k_d}^\dagger + \hat{a}_{k_d}\big)\right) \cdots \left(\sum_{k_2,k_1=1}^{N} A_{2k_2}A_{1k_1}\hat{a}_{k_2}^\dagger\hat{a}_{k_1}^\dagger\right)|\text{vac}\rangle. \tag{A10}$$

Henceforth, we consider the even- and odd-d cases separately. First, assuming d is even, we can reapply the result in Eq. (A9) to the rest of the pairs of summation terms in Eq. (A10), which yields

$$|\Psi_{1,\text{alt}}(A)\rangle = \left(\sum_{k_d,k_{d-1}=1}^{N} A_{dk_d}A_{d-1k_{d-1}}\hat{a}_{k_d}^\dagger\hat{a}_{k_{d-1}}^\dagger\right) \cdots \left(\sum_{k_2,k_1=1}^{N} A_{2k_1}A_{1k_1}\hat{a}_{k_2}^\dagger\hat{a}_{k_1}^\dagger\right)|\text{vac}\rangle \tag{A11}$$

$$= \sum_{k_d,\ldots,k_1=1}^{N} A_{dk_d}\cdots A_{1k_1}\hat{a}_{k_d}^\dagger\cdots\hat{a}_{k_1}^\dagger|\text{vac}\rangle. \tag{A12}$$

Alternatively, if d is odd, we have

$$|\Psi_{1,\text{alt}}(A)\rangle = \left(\sum_{k_d=1}^{N} A_{dk_d}\big(\hat{a}_{k_d}^\dagger + \hat{a}_{k_d}\big)\right)\sum_{k_{d-1},\ldots,k_1=1}^{N} A_{d-1k_{d-1}}\cdots A_{1k_1}\hat{a}_{k_{d-1}}^\dagger\cdots\hat{a}_{k_1}^\dagger|\text{vac}\rangle \tag{A13}$$

$$= \sum_{k_d,\ldots,k_1=1}^{N} A_{dk_d}\cdots A_{1k_1}\big(\hat{a}_{k_d}^\dagger\hat{a}_{k_{d-1}}^\dagger\cdots\hat{a}_{k_1}^\dagger + \hat{a}_{k_d}\hat{a}_{k_{d-1}}^\dagger\cdots\hat{a}_{k_1}^\dagger\big)|\text{vac}\rangle \tag{A14}$$

$$= \sum_{k_d,\ldots,k_1=1}^{N} A_{dk_d}\cdots A_{1k_1}\Big(\hat{a}_{k_d}^\dagger\hat{a}_{k_{d-1}}^\dagger\cdots\hat{a}_{k_1}^\dagger + \cancelto{0}{\delta_{k_dk_{d-1}}\hat{a}_{k_{d-2}}^\dagger\cdots\hat{a}_{k_1}^\dagger} - \hat{a}_{k_{d-1}}^\dagger\hat{a}_{k_d}\hat{a}_{k_{d-2}}^\dagger\cdots\hat{a}_{k_1}^\dagger\Big)|\text{vac}\rangle \tag{A15}$$

$$= \sum_{k_d,\ldots,k_1=1}^{N} A_{dk_d}\cdots A_{1k_1}\Big(\hat{a}_{k_d}^\dagger\hat{a}_{k_{d-1}}^\dagger\cdots\hat{a}_{k_1}^\dagger - \cancelto{0}{\hat{a}_{k_{d-1}}^\dagger\delta_{k_dk_{d-2}}\hat{a}_{k_{d-3}}^\dagger\cdots\hat{a}_{k_1}^\dagger} + \cancelto{0}{\hat{a}_{k_{d-1}}^\dagger\hat{a}_{k_{d-2}}^\dagger\hat{a}_{k_d}\hat{a}_{k_{d-3}}^\dagger\cdots\hat{a}_{k_1}^\dagger}\Big)|\text{vac}\rangle \tag{A16}$$

$$= \sum_{k_d,\ldots,k_1=1}^{N} A_{dk_d}\cdots A_{1k_1}\hat{a}_{k_d}^\dagger\cdots\hat{a}_{k_1}^\dagger|\text{vac}\rangle, \tag{A17}$$

where we have applied the fermionic commutation relation in Eq. (A14) and matrix orthogonality in Eqs. (A15) and (A16). Hence, by combining the even Eq. (A12) and odd Eq. (A17) results, we have established the equivalence between the alternative definition in Eq. (A4) and the original definition in Eq. (A1).

APPENDIX B: PROOF OF ANTICOMMUTATION RELATIONS

Here, we shall show that $\hat{p}_k = \hat{a}_k^\dagger + \hat{a}_k$ has the desired anticommutation relation $\{\hat{p}_i, \hat{p}_j\} = 2\delta_{ij}\mathbf{I}$:

$$\{\hat{p}_i, \hat{p}_j\} = \{\hat{a}_i^\dagger + \hat{a}_i, \hat{a}_j^\dagger + \hat{a}_j\} \tag{B1}$$

$$= (\hat{a}_i^\dagger + \hat{a}_i)(\hat{a}_j^\dagger + \hat{a}_j) + (\hat{a}_j^\dagger + \hat{a}_j)(\hat{a}_i^\dagger + \hat{a}_i) \tag{B2}$$

$$= \cancel{\hat{a}_i^\dagger \hat{a}_j^\dagger} + \hat{a}_i \hat{a}_j^\dagger + \hat{a}_i^\dagger \hat{a}_j + \cancel{\hat{a}_i \hat{a}_j} + \cancel{\hat{a}_j^\dagger \hat{a}_i^\dagger} + \hat{a}_j \hat{a}_i^\dagger + \hat{a}_j^\dagger \hat{a}_i + \cancel{\hat{a}_j \hat{a}_i} \tag{B3}$$

$$= \hat{a}_i \hat{a}_j^\dagger + \hat{a}_i^\dagger \hat{a}_j + \hat{a}_j \hat{a}_i^\dagger + \hat{a}_j^\dagger \hat{a}_i \tag{B4}$$

$$= 2\delta_{ij} I \quad \text{(shown)}. \tag{B5}$$

Next, we shall show that $\hat{p}_\mu^{(L)} = \bigotimes_{r=1}^{\mu-1} \hat{Z}_{rL} \bigotimes_{r'=L(\mu-1)+1}^{\mu L} \hat{X}_{r'}$, used to incorporate L-wise correlation into the Clifford loaders via the Givens-rotation approach, has the desired anticommutation relation $\{\hat{p}_\mu^{(L)}, \hat{p}_\nu^{(L)}\} = 2\delta_{\mu\nu}\mathbf{I}$. We shall split the derivation into two cases, $\mu = \nu$ and $\mu < \nu$. Let us first consider $\mu = \nu$, where

$$2\hat{p}_\mu^{(L)} \hat{p}_\mu^{(L)} = 2 \left(\bigotimes_{r=1}^{\mu-1} \hat{Z}_{rL} \bigotimes_{r'=L(\mu-1)+1}^{\mu L} \hat{X}_{r'} \right) \left(\bigotimes_{s=1}^{\mu-1} \hat{Z}_{sL} \bigotimes_{s'=L(\mu-1)+1}^{\mu L} \hat{X}_{s'} \right) \tag{B6}$$

$$= 2\mathbf{I} \text{ (shown)}. \tag{B7}$$

Second, without loss of generality, let us consider $\mu < \nu$, and we note that $\hat{X}_\mu \hat{Z}_\mu = -i\hat{Y}_\mu$:

$$\hat{p}_\mu^{(L)} \hat{p}_\nu^{(L)} = \left(\bigotimes_{r=1}^{\mu-1} \hat{Z}_{rL} \bigotimes_{r'=L(\mu-1)+1}^{\mu L} \hat{X}_{r'} \right) \left(\bigotimes_{s=1}^{\nu-1} \hat{Z}_{sL} \bigotimes_{s'=L(\nu-1)+1}^{\nu L} \hat{X}_{s'} \right) \tag{B8}$$

$$= -i \left[\bigotimes_{r=(\mu-1)L+1}^{\mu L-1} \hat{X}_r \hat{Y}_{\mu L} \bigotimes_{r'=\mu+1}^{\nu-1} \hat{Z}_{r'L} \bigotimes_{r''=(\nu-1)L+1}^{\nu L} \hat{X}_{r''} \right] \tag{B9}$$

Therefore, by noting $\hat{Z}_\mu \hat{X}_\mu = i\hat{Y}_\mu$ we then have

$$\left\{ \hat{p}_\mu^{(L)}, \hat{p}_\nu^{(L)} \right\} = \hat{p}_\mu^{(L)} \hat{p}_\nu^{(L)} + \hat{p}_\nu^{(L)} \hat{p}_\mu^{(L)} \tag{B10}$$

$$= -i \left[\bigotimes_{r=(\mu-1)L+1}^{\mu L-1} \hat{X}_r \hat{Y}_{\mu L} \bigotimes_{r'=\mu+1}^{\nu-1} \hat{Z}_{r'L} \bigotimes_{r''=(\nu-1)L+1}^{\nu L} \hat{X}_{r''} \right]$$

$$+ i \left[\bigotimes_{s=(\mu-1)L+1}^{\mu L-1} \hat{X}_s \hat{Y}_{\mu L} \bigotimes_{s'=\mu+1}^{\nu-1} \hat{Z}_{s'L} \bigotimes_{s''=(\nu-1)L+1}^{\nu L} \hat{X}_{s''} \right] \tag{B11}$$

$$= 0 \quad \text{(shown)}. \tag{B12}$$

APPENDIX C: EVALUATION OF THE SLATER DETERMINANT AND *L*-WISE CORRELATED *ANSATZ* USING CLIFFORD LOADERS

In the main text, we proposed to construct Clifford loaders $\hat{C}$ using Givens rotation to prepare the Slater determinant $|\Psi_1(A)\rangle$ as follows:

$$|\Psi_1(A)\rangle = \prod_{l=1}^{d} \hat{C}(\vec{A}_l)|\text{vac}\rangle. \tag{C1}$$

We want to show that Eq. (C1) can be mathematically evaluated using geometric algebra, also known as real Clifford algebra. We define a Clifford loader $\hat{C}(\vec{x})$ for a given normalized size-N vector $\vec{x}$ as a linear combination of anticommuting operators $\hat{p}_r$ as follows:

$$\hat{C}(\vec{x}) = \sum_{\mu=1}^{N} x_\mu \hat{p}_\mu. \tag{C2}$$

A geometric product of two Clifford loaders $\hat{C}(\vec{x})\hat{C}(\vec{y})$ for any two normalized size-N vectors $\vec{x}$ and $\vec{y}$ is defined as

$$\hat{C}(\vec{x})\hat{C}(\vec{y}) = \hat{C}(\vec{x}) \cdot \hat{C}(\vec{y}) + \hat{C}(\vec{x}) \wedge \hat{C}(\vec{y}), \tag{C3}$$

where $\cdot$ and $\wedge$ refer to the standard inner dot and exterior wedge products, respectively. Substituting the definition in Eq. (C2) into Eq. (C3), we have

$$\hat{C}(\vec{x})\hat{C}(\vec{y}) = \sum_{r=1}^{N} x_r y_r (\hat{p}_r \cdot \hat{p}_r) + \sum_{\mu,\nu=1}^{N} x_\mu y_\nu (\hat{p}_\mu \wedge \hat{p}_\nu). \tag{C4}$$

In this work, we shall consider only orthogonal and normalized size-N vectors $\vec{A}_l$ for $l = 1, 2, \ldots, d$, such that the inner product of any two vectors is zero. As a result, the geometric product of two Clifford loaders is simply equivalent to its exterior product as the first term of Eq. (C4) vanishes under orthogonality. Thus, products of multiple Clifford loaders can be easily written as exterior products of multiple anticommuting operators,

$$\prod_{l=1}^{d} \hat{C}(\vec{A}_l) = \sum_{\mu,\nu,\ldots,r=1}^{N} A_{\mu 1} A_{\nu 2} \cdots A_{rd} \underbrace{(\hat{p}_\mu \wedge \hat{p}_\nu \wedge \cdots \wedge \hat{p}_r)}_{d \text{ operators}}. \tag{C5}$$

We note the following identities of the exterior product:

$$\hat{p}_\mu \wedge \hat{p}_\mu = 0 \tag{C6}$$

and

$$\hat{p}_{\sigma_1} \wedge \hat{p}_{\sigma_2} \wedge \cdots \wedge \hat{p}_{\sigma_d} = \mathrm{sgn}(\sigma)\hat{p}_{B_1} \wedge \hat{p}_{B_2} \wedge \cdots \wedge \hat{p}_{B_d}, \quad \text{(C7)}$$

where we let σ be a permutation of $\{B_1, B_2, \ldots, B_d\}$ for any ordered set B containing d unique integers between 1 and N and B_μ and σ_μ refer to the μth integers of B and σ, respectively. Using identities (C6) and (C7), the sum in Eq. (C5) reduces to

$$\prod_{l=1}^{d} \hat{C}(\vec{A}_l) = \sum_{|B|=d} \sum_{\sigma \in B} \mathrm{sgn}(\sigma) A_{\sigma_1 1} A_{\sigma_2 2} \cdots A_{\sigma_d d} \times (\hat{p}_{B_1} \wedge \hat{p}_{B_2} \wedge \cdots \wedge \hat{p}_{B_d}), \quad \text{(C8)}$$

where the outer sum is over all possible combinations of the ordered set B containing d unique integers between 1 and N and the inner sum is over all possible integer permutations σ of each B. Using the Leibniz-determinant formula for matrix minors

$$\det(A_B) = \sum_{\sigma \in B} \mathrm{sgn}(\sigma) A_{\sigma_1 1} A_{\sigma_2 2} \cdots A_{\sigma_d d}, \quad \text{(C9)}$$

where A_B is a $d \times d$ matrix minor of A whose rows are restricted to B, we have

$$\prod_{l=1}^{d} \hat{C}(\vec{A}_l) = \sum_{|B|=d} \det(A_B) \hat{p}_{B_1} \wedge \hat{p}_{B_2} \wedge \cdots \wedge \hat{p}_{B_d}. \quad \text{(C10)}$$

Hence, by letting the anticommuting operator be

$$\hat{p}_\mu = \hat{a}_\mu^\dagger + \hat{a}_\mu \quad \text{(C11)}$$

and applying the product of d Clifford loaders (C10) to a vacuum state $|\mathrm{vac}\rangle$, we obtain the alternative expression of the Slater determinant,

$$\prod_{l=1}^{d} \hat{C}(\vec{A}_l)|\mathrm{vac}\rangle = \sum_{|B|=d} \det(A_B)|B\rangle, \quad \text{(C12)}$$

where $|B\rangle$ denotes a Fock state whose occupied modes are indexed by B.

Next, we consider extending the application of Clifford loaders to prepare L-wise correlated *Ansatz* states, where $L = 1$ reduces to the Slater-determinant case. The idea is to use a new set of anticommuting operators $\hat{p}_\mu^{(L)}$ that contains non-particle-preserving multibody Fock operators for the Clifford loaders in Eq. (C2). In the main text, under the Jordan-Wigner mapping, we modify the anticommuting operator $\hat{p}_\mu = \bigotimes_{r=1}^{\mu-1} \hat{Z}_r \hat{X}_\mu$ in Eq. (C11) used to prepare the Slater determinant above to

$$\hat{p}_\mu^{(L)} = \bigotimes_{r=1}^{\mu-1} \hat{Z}_{rL} \bigotimes_{r'=L(\mu-1)+1}^{\mu L} \hat{X}_{r'} \quad \text{(C13)}$$

to apply L-wise correlation. This modified operator $\hat{p}_\mu^{(L)}$ has L Pauli-X terms and μ Pauli-Z terms with modulo L indexes such that $\{\hat{p}_\mu^{(L)}, \hat{p}_\nu^{(L)}\} = 2\delta_{\mu\nu}\mathbf{I}$. For example, the $L = 2$ pairwise correlated anticommuting operators are given as $\hat{p}_\mu^{(2)} = \hat{Z}_2\hat{Z}_4\hat{Z}_6 \cdots \hat{Z}_{2\mu-2}\hat{X}_{2\mu-1}\hat{X}_{2\mu}$. In terms of Fermionic creation and annihilation operators, Eq. (C13) maps back to

$$\hat{p}_\mu^{(L)} = \begin{cases} \bigotimes_{r=1}^{\mu-1}(\mathbf{I} - 2\hat{a}_{rL}^\dagger \hat{a}_{rL}) \bigotimes_{r'=L(\mu-1)+1}^{\mu L} [\hat{a}_{r'}^\dagger + (-1)^{r'} \hat{a}_{r'}] & \text{if } L \text{ is even,} \\ -\bigotimes_{r=1 \notin L\mathbb{Z}}^{L(\mu-1)-1}(\mathbf{I} - 2\hat{a}_r^\dagger \hat{a}_r) \bigotimes_{r'=L(\mu-1)+1}^{\mu L} [\hat{a}_{r'}^\dagger + (-1)^{r'-L(\mu-1)-1} \hat{a}_{r'}] & \text{if } L \text{ is odd,} \end{cases} \quad \text{(C14)}$$

where the r index in the odd-L case increments with size 1 from 1 to $L(\mu - 1) - 1$ but skips every index that is a multiple of L. Here, we note that in Eq. (C14), all fermionic terms in normal ordered form that contain any annihilation operators will vanish when acted upon by a vacuum state and fermionic terms that contain only creation operators will survive. Thus, by substituting Eq. (C14) into the product of $\frac{d}{L}$ Clifford loaders in Eq. (C10) and applying it to a vacuum state $|\mathrm{vac}\rangle$, we obtain an expression of the L-wise correlated *Ansatz* state up to an unobservable global phase,

$$\prod_{l=1}^{\frac{d}{L}} \hat{C}_L(\vec{G}_l)|\mathrm{vac}\rangle \simeq \sum_{|B'|=\frac{d}{L}} \det(G_{B'})|B'_L\rangle, \quad \text{(C15)}$$

where the sum is over all possible combinations of ordered set B' containing $\frac{d}{L}$ unique integers between 1 and $\frac{N}{L}$, $G_{B'}$ is a $\frac{d}{L} \times \frac{d}{L}$ matrix minor of G whose rows are restricted to B', $B'_L = \{L(j-1)+1, L(j-1)+2, \ldots, Lj | j \in B'\}$, and $|B'_L\rangle$ denotes an N-mode Fock basis whose occupied modes are indexed by B'_L.

APPENDIX D: GIVENS-ROTATION GATE AND ITS DECOMPOSITION FOR THE L-WISE CORRELATED *ANSATZ* STATE

The Givens-rotation gate is defined in the main text as

$$\hat{U}_{\mu\nu}^{(L)}(\theta) = \exp\left[\theta \hat{p}_\mu^{(L)} \hat{p}_\nu^{(L)}\right], \quad \text{(D1)}$$

where, with the use of anticommuting operators in Eq. (C13), it becomes

$$\hat{U}_{\mu\nu}^{(L)}(\theta) = \exp\left[-i\theta \bigotimes_{r=L(\mu-1)+1}^{\mu L-1} \hat{X}_r \hat{Y}_{\mu L} \bigotimes_{r'=L(\nu-1)+1}^{\nu L} \hat{X}_{r'} \bigotimes_{r''=\mu+1}^{\nu-1} \hat{Z}_{r''L}\right]. \quad \text{(D2)}$$

For example, an $L = 2$ pairwise Givens rotation would be

$$\hat{U}_{\mu\nu}^{(2)}(\theta) = \exp[-i\theta \hat{X}_{2\mu-1}\hat{Y}_{2\mu}\hat{X}_{2\nu-1}\hat{X}_{2\nu}\hat{Z}_{2(\mu+1)} \times \hat{Z}_{2(\mu+2)} \cdots \hat{Z}_{2(\nu-1)}], \quad \text{(D3)}$$

which can easily be decomposed, as shown in Fig. 6, using gate-decomposition techniques from [40]. Therefore, the

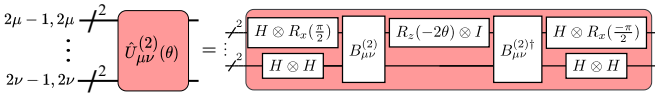

FIG. 6. The pairwise Givens-rotation gate $\hat{U}^{(2)}_{\mu,\nu}$ is decomposed using Pauli-rotation gates R_x, which acts on qubit 2μ that correspond to $\hat{Y}_{2\mu}$, and R_z, which acts on qubit $2\mu-1$, and Hadamard gates H and CNOT ladders $B^{(L)}_{\mu\nu}$ that act on all three qubits in $\{2\mu-1, 2\nu-1, 2\nu\}$ that correspond to $\hat{X}_{2\mu-1}\hat{X}_{2\nu-1}\hat{X}_{2\nu}$, with $B^{(L)}_{\mu\nu}$ also acting on $\nu-\mu$ additional qubits in $\{2\mu, 2(\mu+1), 2(\mu+2), \ldots, 2(\nu-1)\}$. θ is a scalar parameter.

Givens-rotation gate $\hat{U}^{(L)}_{\mu\nu}(\theta)$ used in this work is simply a Pauli-string-rotation gate whose gate decomposition is a generalization of Fig. 6, as shown in Fig. 3(b) of the main text.

APPENDIX E: DERIVATION OF THE TWO-QUBIT GATE-DEPTH SCALING OF THE *L*-WISE CORRELATED QUANTUM CIRCUIT *ANSATZ*

To prepare the L-wise correlated *Ansatz* state $|\Psi_L\rangle$ on a quantum computer under Jordan-Wigner mapping, we apply $\frac{d}{L}$ Clifford loaders $\hat{C}_L$ to an all-zero qubit state. Each Clifford loader $\hat{C}$ has two products of multiple Givens rotations, D_L and $D_L^\dagger$. Each D_L has $\lceil\log_2\frac{N}{L}\rceil$ Givens-rotation gate depth. Each Givens-rotation gate $U^{(L)}_{\mu\nu}$ contains two CNOT ladders $B^{(L)}_{\mu\nu}$ that act on all $2L+\nu-\mu-1$ qubits in $\{L(\mu-1)+1, \ldots, L\mu\}$, $\{L(\mu+1), L(\mu+2), \ldots, L(\nu-1)\}$, and $\{L(\nu-1)+1, \ldots, L\nu\}$. We employ the logarithmic-depth CNOT ladders shown in Fig. 2 in the main text; thus, each CNOT ladder $B^{(L)}_{\mu\nu}$ has a two-qubit gate depth of $\lceil\log_2(2L+\nu-\mu-1)\rceil \approx O(\log_2 N)$. Focusing on all Givens rotations $U^{(L)}_{1,2^s}$ that act on the first qubit in every sublayer $s\in\{1, 2, \ldots, \lceil\log_2\frac{N}{L}\rceil\}$, as shown in Fig. 3(a) in the main text, the overall two-qubit gate depth of the quantum circuit required to prepare the L-wise correlated *Ansatz* state $|\Psi_L\rangle$ is estimated to be

$$\begin{aligned}
&\frac{2d}{L}\sum_{s=1}^{\lceil\log_2\frac{N}{L}\rceil} 2\lceil\log_2(2L+2^s-1-1)\rceil \\
&\leqslant \frac{4d}{L}\sum_{s=1}^{\lceil\log_2\frac{N}{L}\rceil}\log_2(2^{s+\log_2(L)}) &\text{(E1)}\\
&= \frac{4d}{L}\sum_{s=1}^{\lceil\log_2\frac{N}{L}\rceil}[s+\log_2(L)] &\text{(E2)}\\
&= \frac{2d}{L}\left(\left\lceil\log_2^2\frac{N}{L}\right\rceil + (1+2\log_2 L)\left\lceil\log_2\frac{N}{L}\right\rceil\right). &\text{(E3)}
\end{aligned}$$

[1] B. Bauer, S. Bravyi, M. Motta, and G. K.-L. Chan, Quantum algorithms for quantum chemistry and quantum materials science, Chem. Rev. **120**, 12685 (2020).

[2] M. Motta and J. E. Rice, Emerging quantum computing algorithms for quantum chemistry, Wiley Interdiscip. Rev.: Comput. Mol. Sci. **12**, e1580 (2022).

[3] A. J. Daley, I. Bloch, C. Kokail, S. Flannigan, N. Pearson, M. Troyer, and P. Zoller, Practical quantum advantage in quantum simulation, Nature (London) **607**, 667 (2022).

[4] D. S. Abrams and S. Lloyd, Simulation of Many-Body Fermi Systems on a Universal Quantum Computer, Phys. Rev. Lett. **79**, 2586 (1997).

[5] D. S. Abrams and S. Lloyd, Quantum Algorithm Providing Exponential Speed Increase for Finding Eigenvalues and Eigenvectors, Phys. Rev. Lett. **83**, 5162 (1999).

[6] A. Aspuru-Guzik, A. D. Dutoi, P. J. Love, and M. Head-Gordon, Simulated quantum computation of molecular energies, Science **309**, 1704 (2005).

[7] S. Lee, J. Lee, H. Zhai, Y. Tong, A. M. Dalzell, A. Kumar, P. Helms, J. Gray, Z.-H. Cui, W. Liu, M. Kastoryano, R. Babbush, J. Preskill, D. R. Reichman, E. T. Campbell, E. F. Valeev, L. Lin, and G. K.-L. Chan, Evaluating the evidence for exponential quantum advantage in ground-state quantum chemistry Nat. Commun. **14**, 1952 (2023).

[8] K. Bharti, A. Cervera-Lierta, T. H. Kyaw, T. Haug, S. Alperin-Lea, A. Anand, M. Degroote, H. Heimonen, J. S. Kottmann, T. Menke, W.-K. Mok, S. Sim, L.-C. Kwek, and A. Aspuru-Guzik, Noisy intermediate-scale quantum algorithms, Rev. Mod. Phys. **94**, 015004 (2022).

[9] P. Jordan and E. Wigner, Über das Paulische Äquivalenzverbot, Z. Phys. **47**, 631 (1928).

[10] A. Kandala, A. Mezzacapo, K. Temme, M. Takita, M. Brink, J. M. Chow, and J. M. Gambetta, Hardware-efficient variational quantum eigensolver for small molecules and quantum magnets, Nature (London) **549**, 242 (2017).

[11] L. Bittel and M. Kliesch, Training Variational Quantum Algorithms is NP-Hard, Phys. Rev. Lett. **127**, 120502 (2021).

[12] J. Tilly, H. Chen, S. Cao, D. Picozzi, K. Setia, Y. Li, E. Grant, L. Wossnig, I. Rungger, G. H. Booth, and J. Tennyson, The variational quantum egensolver: A review of methods and best practices, Phys. Rep. **986**, 1 (2022).

[13] D. Wecker, M. B. Hastings, N. Wiebe, B. K. Clark, C. Nayak, and M. Troyer, Solving strongly correlated electron models on a quantum computer, Phys. Rev. A **92**, 062318 (2015).

[14] I. D. Kivlichan, J. McClean, N. Wiebe, C. Gidney, A. Aspuru-Guzik, G. K.-L. Chan, and R. Babbush, Quantum Simulation of Electronic Structure with Linear Depth and Connectivity, Phys. Rev. Lett. **120**, 110501 (2018).

[15] F. Arute *et al.*, Hartree-Fock on a superconducting qubit quantum computer, Science **369**, 1084 (2020).

[16] A. Anand, P. Schleich, S. Alperin-Lea, P. W. K. Jensen, S. Sim, M. Díaz-Tinoco, J. S. Kottmann, M. Degroote, A. F. Izmaylov, and A. Aspuru-Guzik, A quantum computing view on unitary coupled cluster theory, Chem. Soc. Rev. **51**, 1659 (2022).

[17] F. A. Evangelista, G. K.-L. Chan, and G. E. Scuseria, Exact parameterization of fermionic wave functions via unitary coupled cluster theory, J. Chem. Phys. **151**, 244112 (2019).

[18] Q. Wang, M. Li, C. Monroe, and Y. Nam, Resource-optimized fermionic local-Hamiltonian simulation on a quantum computer for quantum chemistry, Quantum **5**, 509 (2021).
[19] J. S. Kottmann and A. Aspuru-Guzik, Optimized low-depth quantum circuits for molecular electronic structure using a separable-pair approximation, Phys. Rev. A **105**, 032449 (2022).
[20] H. L. Tang, V. O. Shkolnikov, G. S. Barron, H. R. Grimsley, N. J. Mayhall, E. Barnes, and S. E. Economou, Qubit-ADAPT-VQE: An Adaptive Algorithm for Constructing Hardware-Efficient Ansätze on a Quantum Processor, PRX Quantum **2**, 020310 (2021).
[21] T. E. O'Brien *et al.*, Purification-based quantum error mitigation of pair-correlated electron simulations, arXiv:2210.10799.
[22] R. N. Tazhigulov, S.-N. Sun, R. Haghshenas, H. Zhai, A. T. Tan, N. C. Rubin, R. Babbush, A. J. Minnich, and G. K.-L. Chan, Simulating Models of Challenging Correlated Molecules and Materials on the Sycamore Quantum Processor, PRX Quantum **3**, 040318 (2022).
[23] V. E. Elfving, B. W. Broer, M. Webber, J. Gavartin, M. D. Halls, K. P. Lorton, and A. Bochevarov, How will quantum computers provide an industrially relevant computational advantage in quantum chemistry? arXiv:2009.12472.
[24] B. Nagy and F. Jensen, in *Reviews in Computational Chemistry* (John Wiley & Sons, Ltd., 2017), Vol. 30, pp. 93–149.
[25] J. Romero, R. Babbush, J. R. McClean, C. Hempel, P. J. Love, and A. Aspuru-Guzik, Strategies for quantum computing molecular energies using the unitary coupled cluster ansatz, Quantum Sci. Technol. **4**, 014008 (2018).
[26] J. M. Arrazola, O. Di Matteo, N. Quesada, S. Jahangiri, A. Delgado, and N. Killoran, Universal quantum circuits for quantum chemistry, Quantum **6**, 742 (2022).
[27] G.-L. R. Anselmetti, D. Wierichs, C. Gogolin, and R. M. Parrish, Local, expressive, quantum-number-preserving VQE ansätze for fermionic systems, New J. Phys. **23**, 113010 (2021).
[28] Y. S. Yordanov, D. R. M. Arvidsson-Shukur, and C. H. W. Barnes, Efficient quantum circuits for quantum computational chemistry, Phys. Rev. A **102**, 062612 (2020).
[29] I. Magoulas and F. A. Evangelista, CNOT-efficient circuits for arbitrary rank many-body fermionic and qubit excitations, J. Chem. Theory Comput. **19**, 822 (2023).
[30] C. H. Chee, A. M. Mak, D. Leykam, P. K. Barkoutsos, and D. G. Angelakis, Computing electronic correlation energies using linear depth quantum circuits, arXiv:2207.03949.
[31] I. Kerenidis and A. Prakash, Quantum machine learning with subspace states, arXiv:2202.00054.
[32] G. W. Stewart, Computing the CS decomposition of a partitioned orthonormal matrix, Numer. Math. **40**, 297 (1982).
[33] E. S. Gawlik, Y. Nakatsukasa, and B. D. Sutton, A backward stable algorithm for computing the CS decomposition via the polar decomposition, SIAM J. Matrix Anal. Appl. **39**, 1448 (2018).
[34] S. Johri, S. Debnath, A. Mocherla, A. Singk, A. Prakash, J. Kim, and I. Kerenidis, Nearest centroid classification on a trapped ion quantum computer, npj Quantum Inf. **7**, 122 (2021).
[35] K. Wan, W. J. Huggins, J. Lee, and R. Babbush, Matchgate shadows for fermionic quantum simulation, arXiv:2207.13723.
[36] G. Ortiz, J. E. Gubernatis, E. Knill, and R. Laflamme, Quantum algorithms for fermionic simulations, Phys. Rev. A **64**, 022319 (2001).
[37] Z. Jiang, K. J. Sung, K. Kechedzhi, V. N. Smelyanskiy, and S. Boixo, Quantum Algorithms to Simulate Many-Body Physics of Correlated Fermions, Phys. Rev. Appl. **9**, 044036 (2018).
[38] A. Vourdas, Exterior calculus and fermionic quantum computation, J. Phys. A **51**, 445301 (2018).
[39] I. Kerenidis, J. Landman, and N. Mathur, Classical and quantum algorithms for orthogonal neural networks, arXiv:2106.07198.
[40] J. D. Whitfield, J. Biamonte, and A. Aspuru-Guzik, Simulation of electronic structure Hamiltonians using quantum computers, Mol. Phys. **109**, 735 (2011).
[41] M. Kjaergaard, M. E. Schwartz, J. Braumüller, P. Krantz, J. I.-J. Wang, S. Gustavsson, and W. D. Oliver, Superconducting qubits: Current state of play, Annu. Rev. Condens. Matter Phys. **11**, 369 (2020).
[42] C. D. Bruzewicz, J. Chiaverini, R. McConnell, and J. M. Sage, Trapped-ion quantum computing: Progress and challenges, Appl. Phys. Rev. **6**, 021314 (2019).
[43] J. M. L. Martin, Ab initio total atomization energies of small molecules — Towards the basis set limit, Chem. Phys. Lett. **259**, 669 (1996).
[44] A. Halkier, T. Helgaker, P. Jørgensen, W. Klopper, and J. Olsen, Basis-set convergence of the energy in molecular Hartree–Fock calculations, Chem. Phys. Lett. **302**, 437 (1999).
[45] P. R. Spackman and A. Karton, Estimating the CCSD basis-set limit energy from small basis sets: Basis-set extrapolations vs additivity schemes, AIP Adv. **5**, 057148 (2015).
[46] C. Plascencia, J. Wang, and A. K. Wilson, Importance of the ligand basis set in ab initio thermochemical calculations of transition metal species, Chem. Phys. Lett. **685**, 496 (2017).
[47] P. Virtanen *et al.*, SciPy 1.0: Fundamental algorithms for scientific computing in Python, Nat. Methods **17**, 261 (2020).
[48] Q. Sun, T. C. Berkelbach, N. S. Blunt, G. H. Booth, S. Guo, Z. Li, J. Liu, J. D. McClain, E. R. Sayfutyarova, S. Sharma, S. Wouters, and G. K.-L. Chan, PySCF: The Python-based simulations of chemistry framework, Wiley Interdiscip. Rev.: Comput. Mol. Sci. **8**, e1340 (2018).
[49] V. Bergholm *et al.*, PennyLane: Automatic differentiation of hybrid quantum-classical computations, arXiv:1811.04968.